

# A promising on-off Chemosensor Based on Manganese(II) Complex of a Xanthene Ligand as an Easily Commercially Available Dye for the Detection of Cysteine in Biological Samples

Hossein Tavallali,\* Hesamadin Haghdan

Department of Chemistry, Payame Noor University 19395-4697 Tehran, Islamic Republic of Iran

Received: 30 August 2024

Accepted: 6 September 2024

DOI: [10.30473/ijac.2024.72220.1306](https://doi.org/10.30473/ijac.2024.72220.1306)

## Abstract

A novel colorimetric chemosensor for naked-eye detection and determination of  $Mn^{2+}$  and cysteine (Cys) based on indicator displacement assay (IDA) was designed using bromo pyrogallol red (BPR). The indicator exchange occurred between BPR and Cys by the addition of Cys to the  $Mn(BPR)$  complex, which is accomplished by an immediate visible color change from purple to magenta, in EtOH/HEPES buffer  $10.0 \text{ mmol L}^{-1}$ , pH 9.3 (1:4 v/v). The proposed method exhibits a  $0.02 \text{ } \mu\text{mol L}^{-1}$  detection limit and good linearity in the range of  $0.11\text{--}2.87 \text{ } \mu\text{mol L}^{-1}$  for cysteine amino acid. Additionally, the absorption and color change obtained in this chemosensor operate as an "IMPLICATION" logic gate considering  $Mn^{2+}$  and Cys as inputs. Eventually, based on such a fast, reversible, and reproducible signal, a molecular-scale sequential memory unit was designed to display "keypad lock" behavior. The developed chemosensor presented satisfactory repeatability, good precision, and successful application for the selective determination of Cys in human biological fluids. Furthermore, the method's accuracy was evaluated by comparing the results obtained from the proposed method and those from the reference method.

## Keywords

Indicator Displacement Assay (IDA); Colorimetric Chemosensor; Manganese(II); Cysteine; Bromo Pyogallol Red (BPR); Molecular Keypad Lock.

## 1. INTRODUCTION

Manganese as a trace element plays a role in many physiological processes of the human body [1, 2]. Environment and our food and can consume an average of  $5 \text{ mg/kg}$  per day [3]. Deficiency or excessive amounts of manganese ions significantly affect human health [4]. Its deficiency leads to impaired growth and development, skeletal abnormalities, and immune system function, while excessive exposure to Mn leads to movement disorders, cognitive impairment, and psychiatric symptoms [5, 6]. On the Toxic Release Inventory (TRI) and the Occupational Safety and Health Administration (OSHA), manganese is recognized as a hazardous chemical and an air pollutant [7]. Therefore, there is an urgent need to develop methods to identify manganese ions that can be distinguished from other metal ions, especially calcium ions [8]. On the other hand, manganese ions are quite stable in environmental samples.

Therefore, many efforts have been made to develop different methods for measuring manganese ions with high sensitivity and accuracy [8, 9]

Amino acids are essential moderators of biological processes and play a vital role in the body's metabolism, therefore, in recent decades, the use of colorimetric chemosensors and biosensors for their accurate and rapid determination has received much attention [10]. L-cysteine is involved in many processes such as detoxification of heavy metals [11], the construction of proteins and their folding stability, the biogenesis of iron-sulfur (Fe-S) groups [12], which is important in respiration, and also in the production of taurine, which is important for mitochondrial function and osmolarity control [13]. The cell is essential, it plays a vital role. In addition, its antioxidant properties balance blood sugar levels and digestive function in living organisms. Therefore, some

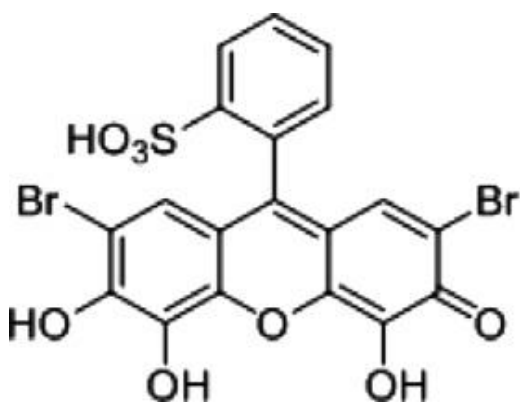
\* Corresponding author:

H. Tavallali; E-mail: Tavallali@pnu.ac.ir, Tavallali@yahoo.com

diseases such as liver and skin, Alzheimer's, neurotoxicity, growth delay in children, low immunity, cancer in severe cases, etc., cause its deficiency or change in its levels [14].

Many analytical methods are used to determine cysteine, such as gas chromatography (GC), capillary electrophoresis (CE), high performance liquid chromatography (HPLC), mass spectrometry, and electrochemical methods [15-17]. The presented methods have disadvantages such as high usage cost and time-consuming complex processes. On the other hand, colorimetric methods have some advantages, such as ease of use, selectivity and high sensitivity, low cost and fast [18-20].

In many cases, chemical sensors synthesized with organic compounds have been used for identification. The synthesis steps are hard and boring. Chemical sensors based on commercial compounds have compensated these disadvantages [21]. Bromopyrogallol red (BPR) is one such chemical sensor (Scheme 1). The structure of BPR includes a xanthen part, benzene sulfonic acid group and -OH functional groups and has a very good ability to form complexes with metal cations [22-25]. BPR can detect various analytes such as anions, amino acids by index displacement assay (IDA). IDA consists of two steps, first the receptor forms a complex with a metal ion, which is associated with a color change, and then the increase of the competitive analyte causes the metal ion to move from the receptor and form a new complex with it [26]. This approach has attracted the attention of many researchers due to its simplicity and ease, but very few papers have been presented on colorimetric chemical sensors for the detection of analytes by IDA approach [18-20, 27, 28].



**Scheme 1.** The molecular structure of Bromo pyrogallol red [2-(2,7-dibromo-4,5,6-trihydroxy-3-oxo-3H-xanthen-9-yl)benzenesulphonic acid, BPR].

In this current proposed method, a new manganese(II) complex with BPR, BPR-Mn<sup>2+</sup> ensembles, was proposed for highly sensitive and selective detection of Cys in EtOH/HEPES buffer

10.0 mmol L<sup>-1</sup>, pH 9.3 (1:4 v/v) solution. Based on titration data in solvent medium, L-cysteine is the best chelator for manganese (II). Complexes of amino acids with Mn(II) should be better models for biological systems, since it is generally believed that Mn porphyrins are not found in chloroplasts and Mn-containing superoxide dismutase. This report deals with the coordination affinity of various amino acids and similar oxygen-nitrogen donor compounds with manganese(II) [29].

Herein, we use BPR as a colorimetric receptor for Mn<sup>2+</sup> ions, and then the BPR-Mn complex was used as a chemosensing ensemble for the detection of Cys via indicator displacement assays approach. Selective detection of Cys was attained based on the competition between the indicator and Cys for binding to Mn<sup>2+</sup>. After adding an appropriate amount of Cys into the BPR- Mn<sup>2+</sup> solution, due to the high affinity of Cys toward Mn<sup>2+</sup>, straightway BPR was displaced with Cys, and BPR was released into the solution, and a color change appeared. It was represented that the sensing system displays good colorimetric response towards Cys in EtOH/HEPES buffer 10.0 mmol L<sup>-1</sup>, pH 9.3 (1:4 v/v) solution. The analogous affinity of the Mn<sup>2+</sup> receptor toward Cys compared to the BPR receptor endowed our colorimetric method with a molecule-exchange signal, especially without further complicated synthetic and treating methods to goodly meet the simple and practical fashion of the current colorimetric sensor. The feasibility of such a colorimetric indicator displacement assay for cysteine determination will be investigated in the following section. Furthermore, molecular logic gates have been developed based on the idea that chemically encoded information as the input is converted into absorbance signals as the output. In this work, the designed colorimetric chemosensor exhibits a logic gate (IMPLICATION) involving Mn<sup>2+</sup>, Cys, and BPR. The proposed chemosensor represented the molecular-level logic behavior employing on the correct sequential addition of Mn<sup>2+</sup> and Cys as inputs, mimicking the "security keypad lock function with the A<sub>545nm</sub> output. Additionally, besides the reversibility of the sensor in solution media, ascertaining the promising application of the present method in biological analysis. Furthermore, the method's accuracy was evaluated by comparing the results obtained from the proposed method and those from the reference method. This chemical system was also used to create and design a security keypad lock on the correct sequential addition of Mn<sup>2+</sup> and Cys.

## 2. EXPERIMENTAL

### 2.1. Materials and equipment

All the reagents, Bromo pyrogallol red [2-(2,7-dibromo-4,5,6-trihydroxy-3-oxo-3H-xanthen-9-

yl) benzene sulphonic acid, BPR], metal salts (nitrate), amino acids, and solvents used were purchased from Merck. The chemicals used were all of the analytical grades. A Perkin Elmer Lambda 14 spectrophotometer obtained UV-Vis absorption spectra using a quartz cuvette. The pH of the solutions was measured using a Jenway 3510 pH meter calibrated with Merck standard buffer solutions at pH 4.0 and 10.0.

### 2.2. Preparation of buffer solution:

A pH effect experiment was conducted with buffer solutions of different pH ranges from 3.0 to 11.0. These buffer solutions included: acetic acid/NaOH (pH 3.0–4.0), MES/NaOH (pH 5.0–6.0), HEPES/NaOH (pH 9.3–10.0), and CABS (pH 10.0–11.0).

#### How to prepare samples of buffer solutions:

**0.1 mol L<sup>-1</sup> Acetate Buffer pH=5.6:** Add 7.721 g of Sodium Acetate and 352.5 mg of Acetic Acid to 800 mL of deionized water. Adjust solution to desired pH by HCl or NaOH and add deionized until the volume is 1.0 L.

**1.0 mol L<sup>-1</sup> HEPES pH=7.5:** Add 238.3 g of HEPES free acid to 800 mL of deionized water. Adjust solution to desired pH by 10 mol L<sup>-1</sup> NaOH and add deionized until the volume is 1.0 L.

**0.5 mol L<sup>-1</sup> MES pH=6.0:** Add 97.62 g of MES free acid to 800 mL of deionized water. Starting pH for 0.5 mol L<sup>-1</sup> MES solution is 3.23 for 1 L of 0.5 mol L<sup>-1</sup> MES, 13.6 mL of 10 mol L<sup>-1</sup> NaOH is needed to adjust the pH to 6.0. and add deionized until the volume is 1.0 L.

**0.5 mol L<sup>-1</sup> CAPS pH=10.5:** Add 110.66 g of CAPS to 800 mL of deionized water. Adjust solution to desired pH by 10 mol L<sup>-1</sup> NaOH and add deionized until the volume is 1.0 L.

### 2.3. Preparation of Solutions

The Na<sup>+</sup>, K<sup>+</sup>, Co<sup>2+</sup>, Mn<sup>2+</sup>, Cr<sup>3+</sup>, Ca<sup>2+</sup>, Li<sup>+</sup>, Ba<sup>2+</sup>, Bi<sup>3+</sup>, Mg<sup>2+</sup>, Fe<sup>2+</sup>, Fe<sup>3+</sup>, Cd<sup>2+</sup>, Ag<sup>+</sup>, Pb<sup>2+</sup>, and Al<sup>3+</sup> in 1 × 10<sup>-2</sup> mol L<sup>-1</sup> stock solutions have been prepared in deionized water. Amino acids include L- lysine (Lys), Glutamic acid (Glu), L-serine (Ser), L-threonine (Thr), glutamine (Gln), L-valine (Val), L-Isoleucine (Ile), L-proline (Pro), L-tyrosine (Tyr), L-tryptophan (Trp), L-phenylalanine (Phe), L-cysteine (Cys), L-arginine (Arg), L-glycine (Gly), L-alanine (Ala), L-histidine (His), Leucine (Leu), aspartic acids (Asp), Asparagine (Asn) and L-methionine (Met) in 1 × 10<sup>-2</sup> mol L<sup>-1</sup> stock solutions have been prepared in deionized water. The 1 × 10<sup>-2</sup> mol L<sup>-1</sup> BPR solutions were prepared using EtOH/HEPES buffer 10.0 mmol L<sup>-1</sup>, pH 9.3 (1:4 v/v). Then the standard solution (3 × 10<sup>-5</sup> mol L<sup>-1</sup>) daily basis by diluting the stock solution with deionized water. After that, information about the BPR and Mn<sup>2+</sup> complex was obtained by titration of BPR (3 × 10<sup>-5</sup> mol L<sup>-1</sup>) and Mn<sup>2+</sup> (1 × 10<sup>-2</sup>

mol L<sup>-1</sup>), in a similar way to the information about the BPR-Mn-Cys through the titration of the complex BPR-Mn with Cys (1 × 10<sup>-2</sup> mol L<sup>-1</sup>) and investigations of the UV-Vis spectrum and their optical response were done.

### 2.4. Procedure of pH optimization

2.5 mL of BPR working solutions (3.0 × 10<sup>-5</sup> mol L<sup>-1</sup>) were transferred to the cuvette, next, we adjusted the pH values by adding buffers from 3 to 11. The pHs in the range of 3.0–4.0, 4.5–7.0, 7.0–10.0, and 10.0–11.4 were respectively adjusted with buffer solutions of CH<sub>3</sub>COOH/NaOH, MES/NaOH, HEPES, and CABS. Upon achieving the desired pH values, 30.0 μmol L<sup>-1</sup> of Mn<sup>2+</sup> solution was transferred to each cuvette, and the UV-Vis spectra were recorded. After that, 40.0 μmol L<sup>-1</sup> of Arg solution was transferred to each cuvette, and the UV-Vis spectra were recorded.

### 2.5. Preparation of environmental and biological samples

This study was approved by the Institutional Review Board of Shiraz Medical College. The proposed method was applied to determining cysteine in biological fluids, including human urine and blood plasma. Human plasma was prepared as follows: 5.0 mL of human blood was transferred into a washed polyethylene tube. After the addition of sodium heparin 75 USP units, the sample was centrifuged at 2000g for 15 min. Then, the plasma was collected in a washed and sterilized tube. The urine samples, from adults, were collected in a sterilized polyethylene tube. To measure manganese ions in real samples, drinking water samples were collected from Payam Noor University, Shiraz, Iran, and running water from Qara Aghaj River in Firozabad, Iran. The samples are made according to our previous publications [30].

### 2.6. Using a standard method for cysteine determination

Urine and plasma samples were used directly without the need for pretreatment or adding other reagents. HPLC analysis of plasma samples was performed using 5,5'-dithio-bis nitrobenzoic acid (DTNB) following the known procedure [31]. The plasma samples were derivatized with 10 mmol L<sup>-1</sup> DTNB at room temperature in pH 7.2 for 10 min, filtered, and injected into the HPLC. The mobile phase was composed of methanol (A) and the aqueous solution of KH<sub>2</sub>PO<sub>4</sub> 100 mmol L<sup>-1</sup> (B) with a ratio of 12:88 (A/B v/v). The analysis was performed using 20 μL injection volume, flow rate of 1.2 mL/min, and UV detection wavelength of 230 nm. The concentrations of the samples added were calculated by using the molecular weight of cysteine and compared with the values obtained

using the proposed procedure and reference method and their differences were estimated by student *t*-test.

### 2.7. General procedures of spectra detection

All titration measurements were done at 298 K and EtOH/HEPES buffer 10.0 mmol L<sup>-1</sup>, pH 9.3 (1:4 v/v) media. Titration measurements using a UV-Vis spectrophotometer instrument showed the same result as naked-eye detection. Stock solutions of BPR were prepared in EtOH/HEPES buffer 10.0 mmol L<sup>-1</sup>, pH 9.3 (1:4 v/v) medium. Before spectroscopic measurements, the solution was freshly prepared by diluting the high-concentration stock solution to the corresponding solution (3.0×10<sup>-5</sup> mol L<sup>-1</sup>). A 2.5 mL of BPR solution was filled in a quartz cell of 1 cm optical path length, and Mn<sup>2+</sup> solution was added into a quartz cell gradually by using a micro-syringe. The volume of cationic stock solution added was less than 100 μL to keep the total volume of the testing solution without obvious change. The BPR-Mn<sup>2+</sup> solution was used for Cys and other amino acid sensing.

For determination of Mn<sup>2+</sup> with BPR dye, 2.5 mL of PAR (3.0×10<sup>-5</sup> mol L<sup>-1</sup>) in EtOH/HEPES buffer 10.0 mmol L<sup>-1</sup>, pH 9.3 (1:4 v/v) medium was transferred into the quartz cuvette and the absorption spectra were recorded. After the addition of Mn<sup>2+</sup> (7.8×10<sup>-7</sup>–9.8×10<sup>-5</sup> mol L<sup>-1</sup>) into the BPR solution, a color change from magenta to purple was specified. Changes in the UV-Vis absorption spectrum of BPR upon titrimetric addition of Mn<sup>2+</sup> were used for complexation studies. This complex was used as a chemosensing ensemble for the detection of amino acids in EtOH/HEPES buffer 10.0 mmol L<sup>-1</sup>, pH 9.3 (1:4 v/v) medium.

Then, the proper amount of Cys was directly added to the complex solution, and the UV-Vis spectra and optical responses were evaluated instantly. The absorbance spectra were then recorded immediately, also changes in the UV-Vis absorption spectrum of BPR-Mn<sup>2+</sup> complex upon addition of the appropriate amount of Cys (7.0×10<sup>-8</sup>–5.1×10<sup>-5</sup> mol L<sup>-1</sup>) were used for complexation studies.

## 3. RESULTS AND DISCUSSION

### 3.1. BPR-Mn<sup>2+</sup> complexation studies (naked eye and UV-Vis detection)

It was known that Bromo pyrogallol red [2-(2,7-dibromo-4,5,6-trihydroxy-3-oxo-3H-xanthene-9-yl) benzene sulphonic acid, BPR] includes a xanthene part, benzene sulfonic acid group, and -OH functional groups and has a very good ability to form complexes with metal cations [22-25]. In this respect, it was determined that BPR can react with Mn<sup>2+</sup>. The binding properties of BPR with Mn<sup>2+</sup> were studied by UV-Vis titration experiment.

Fig. 1a on the gradual addition of Mn<sup>2+</sup> (7.8×10<sup>-7</sup>–9.8×10<sup>-5</sup> mol L<sup>-1</sup>) to a BPR solution, the absorption band at 545 nm significantly decreased. It made clear that with an additional small amount of Mn(II) nitrate solution to BPR in EtOH/HEPES buffer 10.0 mmol L<sup>-1</sup>, pH 9.3 (1:4 v/v) medium, which resulted in a color change from magenta to purple (Fig. 1a).

The band intensity of 545 nm was monitored upon the addition of Mn<sup>2+</sup>, which allowed us to determine the complex stability constant. The 1:1 stoichiometry of the complex (BPR: Mn) was established by the Benesi-Hildebrand analysis [32] of the absorption titration data. When assuming a 1: n stoichiometry for the association between BPR and Mn<sup>2+</sup>, the association constant, K<sub>ass</sub>, is given by the following equation (Eq. (1)):

$$\frac{1}{(A_0 - A)} = \frac{1}{(A_0 - A_{max})} \left[ \frac{1}{K_{ass}[Mn^{2+}]^n} + 1 \right] \quad (1)$$

A<sub>0</sub> is the absorbance of BPR without cation, A is the absorbance of BPR obtained with Mn<sup>2+</sup>. A<sub>max</sub> is the saturated absorbance of BPR in the presence of an excess amount of Mn<sup>2+</sup>, and [Mn<sup>2+</sup>] is the concentration of Mn<sup>2+</sup> ion added. As shown in Figure 1b, the plot of 1/(A<sub>0</sub>-A) at 545 nm against 1/[Mn<sup>2+</sup>] shows a linear relationship, indicating that BPR associates with Mn<sup>2+</sup> in a 1:1 stoichiometry (formation of BPR-Mn species) at 545 nm. K<sub>ass</sub> is determined from the intercept/slope to be 2.05(±0.12) × 10<sup>3</sup> mol<sup>-1</sup> L.

The UV-Vis spectroscopy was used to investigate the binding behavior of BPR toward different metal ions. Different metal ions (150.0 μmol L<sup>-1</sup>) were applied (Mentioned in Preparation of Solutions section). As a highly selective probe for the target analyte, a good capacity for resisting disturbance is required. Using UV-Vis absorption spectroscopy, competitive experiments were performed in the presence of potential metal ions. Except for Mn<sup>2+</sup>, the other metal ions (150 μmol L<sup>-1</sup>) did not produce significant absorption changes (Fig. 1c). Among all the tested cations, BPR showed high selectivity toward Mn<sup>2+</sup> ion while interaction with other cations produced insignificant observable change.

In the concentration range of 1.2×10<sup>-6</sup>–7.3×10<sup>-5</sup> mol L<sup>-1</sup>, the UV-Vis absorption had a linear relationship with Mn<sup>2+</sup> concentration. The regression equation was A<sub>545</sub> = 0.6784-0.004C<sub>Mn</sub> (μmol L<sup>-1</sup>) with a correlation coefficient of 0.9984 (Fig. 1d). Based on the titration and linear relationship, the detection limit (3δ/slope) and the quantification limit (10δ /slope) of BPR- toward Mn<sup>2+</sup> were calculated to be 0.3 μmol L<sup>-1</sup> and 1.0 μmol L<sup>-1</sup>, respectively. Fig. 1d shows the absorbance as the concentration of Mn<sup>2+</sup> ranges from 1.2 to 73.0 μmol L<sup>-1</sup>, which is a perfect linear relationship (R<sup>2</sup> = 0.9984). Furthermore, a lower detection limit (1.2 μmol L<sup>-1</sup>) is addressed based on

$3\sigma$ , with comparison to previously reported  $Mn^{2+}$  determination methods [8, 33-37] (Table 1). In the meantime, the assay avoids any indirect, time-consuming problems and is convenient without any labels or complicated operations.

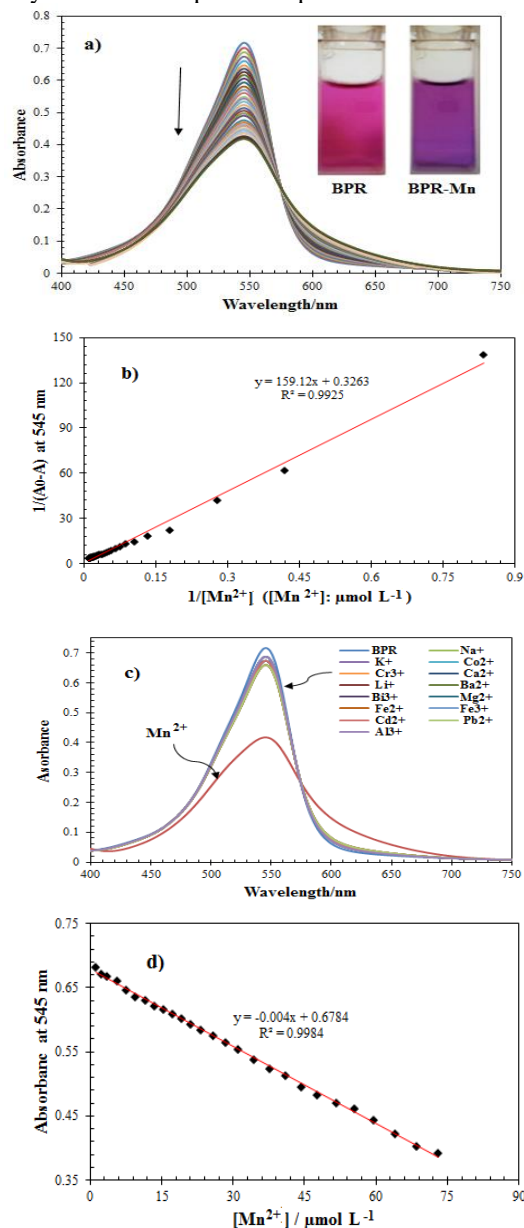


**Fig. 1 a)** UV-Vis spectra of BPR ( $30.0 \mu\text{mol L}^{-1}$ ) upon gradual addition of  $Mn^{2+}$  ( $7.8 \times 10^{-7}$ – $9.8 \times 10^{-5} \text{ mol L}^{-1}$ ), right inset: corresponding color change of BPR upon addition of  $30.0 \mu\text{mol L}^{-1} Mn^{2+}$  in EtOH/HEPES buffer  $10.0 \text{ mmol L}^{-1}$ , pH 9.3 (1:4 v/v), **b)** UV-Vis spectra of BPR ( $30.0 \mu\text{mol L}^{-1}$ ), BPR+  $30 \mu\text{mol L}^{-1}$  of  $Mn^{2+}$  ion BPR+ $150 \mu\text{mol L}^{-1}$  of each cations, in EtOH/HEPES buffer  $10.0 \text{ mmol L}^{-1}$ , pH 9.3 (1:4 v/v), **c)** Benesi-Hildebrand plot ( absorbance at 545 nm) of BPR (the variation of  $1/(A_0-A)$  at 545 nm versus the function of  $1/[Mn^{2+}]$ ) based on 1:1 binding stoichiometry with  $Mn^{2+}$ , **d)** The linearly proportional relationship between the absorbance of BPR solution and the concentration of  $Mn^{2+}$  at 545 nm, in EtOH/HEPES buffer  $10.0 \text{ mmol L}^{-1}$ , pH 9.3 (1:4 v/v).

### 3.2. BPR- $Mn^{2+}$ ensemble for detection of cysteine

It was shown that the BPR- $Mn^{2+}$  complex is a suitable chromogenic chemosensor for amino acid sensing. After the addition of the same amount of 21 amino acids into the solutions of the BPR- $Mn^{2+}$  complex, it appeared that only cysteine can change the color of the BPR- $Mn^{2+}$  complex from purple to magenta selectively and other amino acids could not considerably change the color of the chemosensor solution. Fig. 2a and 2b. Although, change in the visible spectrum was recorded in EtOH/HEPES buffer  $10.0 \text{ mmol L}^{-1}$ , pH 9.3 (1:4 v/v) solution of this chemosensor upon addition of 21 amino acids (Mentioned in Preparation of Solutions section). BPR- $Mn^{2+}$  complex gave a more selective response to cysteine. In this respect, it was determined that BPR can react with  $Mn^{2+}$ . The binding properties of BPR- $Mn^{2+}$  with Cys were studied by UV-Vis titration experiment. Fig. 2c on the gradual addition of Cys ( $7.0 \times 10^{-8}$ – $5.1 \times 10^{-5} \text{ mol L}^{-1}$ ) to a BPR- $Mn^{2+}$  solution, the absorption band at 545 nm significantly decreased. It made clear that with an additional small amount of Cys solution to BPR- $Mn^{2+}$  in EtOH/HEPES buffer  $10.0 \text{ mmol L}^{-1}$ , pH 9.3 (1:4 v/v) medium, which resulted in a color change from purple to magenta (Inset Fig. 2a and 2c).

L-cysteine is a semi-necessary amino acid with the formula  $\text{HOOC-CH}(\text{NH}_2)\text{-CH}_2\text{-SH}$ . It is mostly applied in the medical field whereby it is used to treat arthritis and hardening of the arteries. Furthermore, it can be used to treat lung-related diseases which include bronchitis, emphysema, and tuberculosis. It has a carboxyl group ( $-\text{COOH}$ ) which is the combination of two functional groups that are attached to a single carbon atom, namely hydroxyl ( $-\text{OH}$ ) and carbonyl ( $=\text{O}$ ). It also has an amine group ( $-\text{NH}_2$ ). It is a compound and another functional group can be found in L-cysteine that contains a basic nitrogen atom. The thiol group ( $-\text{SH}$ ) is often involved in enzymatic reactions as a nucleophile. It is highly reactive and susceptible to be oxidized which will turn into cystine. In this work, the thiol group plays an important role as a heavy metal detector because this group has a high affinity toward heavy metal ions [38].

### 3.3. The evaluation of binding stoichiometry of interaction of the [BPR-Mn] complex and Cys

We perused the interaction of Cys and the [BPR-Mn] complex by Ultraviolet-visible spectroscopy. The assessment and analysis of Benesi-Hildebrand plots [32] for the titration data of the absorbance spectra confirmed the 1:1 stoichiometry for [BPR-Mn] complex associated with Cys, so the  $K_{\text{ass}}$  is obtained by the following equation (Eq. (2)):

$$\frac{1}{(A-A_0)} = \frac{1}{(A_{\text{max}}-A_0)} \left[ \frac{1}{K_{\text{ass}}[\text{Cys}]^n} + 1 \right] \quad \text{Eq. (2)}$$

In the above equation,  $A_0$  is the absorbance of the [BPR-Mn] complex when Cys has not been added yet,  $A$  is the absorbance of the [BPR-Mn] complex with the addition of Cys,  $A_{max}$  is the absorbance obtained with the excess amount of Cys,  $[Cys]$  is the concentration of Cys added and  $K_{ass}$  is the association constant ( $L mol^{-1}$ ). The linear-Hilbrand expression indicated the variation of  $1/(A-A_0)$  at 545 nm versus the function of  $1/[Cys]$  in a linear relationship (Fig. 3a). The binding constant ( $K_{ass}$ ) obtained  $1.02(\pm 0.17) \times 10^5 L mol^{-1}$  supported to confirm the 1:1 stoichiometry due to the interaction of the [BPR-Mn] complex and Cys.

The thiol-containing amino acid of cysteine can bind to the  $Mn^{2+}$  ion through the formation of a Mn-S bond with the overall stability constant  $\log K_{ass} > 3.75$  [29]. Since the  $K_{ass}$  of BPR-Mn calculated  $((2.05(\pm 0.12) \times 10^3 L mol^{-1}, \log K_{ass} = 3.31)$  is lower than that of [BPR-Mn]-Cys, this explanation is rational that the association of

Cys with  $Mn^{2+}$  is much more than that of BPR with  $Mn^{2+}$ . Therefore, the indicator displacement is achieved. After addition of in EtOH/HEPES buffer  $10.0 mmol L^{-1}$ , pH 9.3 (1:4 v/v) solution of cysteine into BPR- $Mn^{2+}$  solution, cysteine could competitively coordinate with  $Mn^{2+}$ , resulting in a rapid color change in the BPR- $Mn^{2+}$  solution via a displacement of Cys instead of BPR and producing new Cys- $Mn^{2+}$  (R-SH-Mn) complex, simultaneously BPR deallocated into solution, this makes visible color change from purple to magenta Fig. 2b. Thus, we thought that the added  $Mn^{2+}$  might have captured Cys from the  $Mn(Cys)_n$ , as demonstrated in Scheme 2. The selectivity and sensitivity of BPR- $Mn^{2+}$  complex to Cys using Mn-sulfur affinity were examined. It should be noted that UV-Vis titration of BPR- $Mn^{2+}$  complex in EtOH/HEPES buffer  $10.0 mmol L^{-1}$ , pH 9.3 (1:4 v/v) solution of Cys resulted via indicator displacement assay approach.

**Table 1.** Literature comparison of sensing performance of  $Mn^{2+}$  sensors

Probe Structure	Method	$K_a$	LOD $\mu mol L^{-1}$	Solvent media	Type of matrix	Ref
salicylaldehyde-hydrazine Schiff base	UV-Vis/ FL	$8.50 \times 10^5$	0.36	THF:H <sub>2</sub> O (1:1, v/v)	tap water	[89]
Nitro-PAPS	UV-Vis	$1.21 \times 10^3$	2.23	phosphate buffer	NS	[33]
[Tb <sub>2</sub> (bt dc) <sub>3</sub> (DMF) (H <sub>2</sub> O) <sub>4</sub> ·DMF	FL	$3.53 \times 10^5$	810.00	EtOH	NS	[34]
[Tb <sub>2</sub> (bt dc) <sub>3</sub> (H <sub>2</sub> O) <sub>6</sub> ]	FL	$5.25 \times 10^5$	710.00	EtOH	NS	[34]
Polymer dots	FL/ UV-Vis	-	0.40	PBS buffer	water samples	[35]
N, N-bis((6-(thiophen-3-yl) pyridine-2-yl)methylene)benzene-1,2-diamine	FL	$3.10 \times 10^3$	-	EtOH	water sample	[36]
8-hydroxyjulolidine-9-carboxaldehyde with 2,2-oxybis (ethylamine)	FL/ UV-Vis	$5.02 \times 10^4$	6.03	DMF	NS	[37]
2',7'-Dibromo-3',4',5',6'-tetrahydroxy-1 <i>H</i> -1λ <sup>6</sup> -spiro[[2,1]benzoxathiole-3,9'-xanthene]-1,1-dione	UV-Vis	$2.05 \times 10^3$	0.3	(H <sub>2</sub> O/EtOH , 1:4 v/v)	Water samples	Pesent ed work

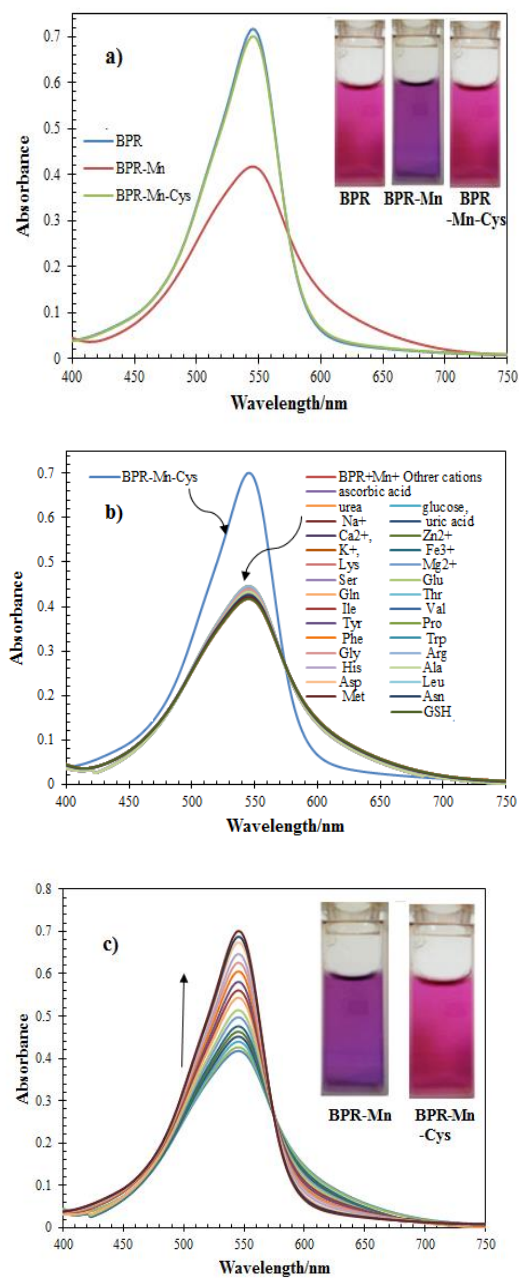
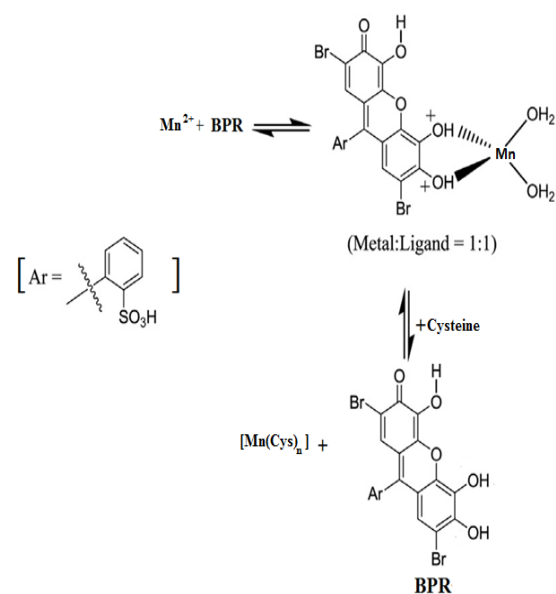


**Fig. 2.** **a)** Reversibility UV-Vis experiment and color changes of BPR ( $30.0 \mu\text{mol L}^{-1}$ ) after the sequential addition of  $\text{Mn}^{2+}$  ( $30.0 \mu\text{mol L}^{-1}$ ) and Cys ( $30.0 \mu\text{mol L}^{-1}$ ) in EtOH/HEPES buffer  $10.0 \text{mmol L}^{-1}$ , pH 9.3 (1:4 v/v), **b)** The UV-Vis absorption changes of receptor (BPR-  $\text{Mn}^{2+}$ ) in EtOH/HEPES buffer  $10.0 \text{mmol L}^{-1}$ , pH 9.3 (1:4 v/v), toward Cys in the presence of amino acids and the interferences of the co-existing substances in biological matrices (including magnesium, zinc, iron(III), potassium, calcium and sodium ions, glucose, urea, uric acid and ascorbic acid) ( $200.0 \mu\text{mol L}^{-1}$ ): BPR- $\text{Mn}^{2+}$  Chemosensor for  $30.0 \mu\text{mol L}^{-1}$  Cys and  $200.0 \mu\text{mol L}^{-1}$  interferences **c)** UV-Vis spectra of BPR ( $30.0 \mu\text{mol L}^{-1}$ ) with combination of  $\text{Mn}^{2+}$  ( $30.0 \mu\text{mol L}^{-1}$ ) upon gradual addition of Cys ( $7.0 \times 10^{-8}$ – $5.1 \times 10^{-5} \text{mol L}^{-1}$ ) in EtOH/HEPES buffer  $10.0 \text{mmol L}^{-1}$ , pH 9.3 (1:4 v/v), inset: corresponding color change of BPR-  $\text{Mn}^{2+}$  upon addition of  $30.0 \mu\text{mol L}^{-1}$  Cys (left to right) in EtOH/HEPES buffer  $10.0 \text{mmol L}^{-1}$ , pH 9.3 (1:4 v/v).



**Scheme 2.** Predicted mechanism of interactions and proposed binding sites between BPR- $\text{Mn}^{2+}$  receptor and cysteine amino acid

This procedure for colorimetric determination of Cys has some conveniences, such as ease of use, selectivity, high sensitivity, low cost, and time conservation. The kinetics for the reaction of BPR and  $\text{Mn}^{2+}$ , and the displacement reaction between the BPR- $\text{Mn}^{2+}$  complex and cysteine were very fast as these reactions reached equilibrium within less than 1 min (Fig. 3b). Therefore, 1 min was chosen as the assay reaction time in all experiments. To improve the sensitivity of the developed bioassay, we used the absorbance at 545 nm, as the response for quantitation. These observations support the sensing mechanism of our method and provide an additional simple approach for detecting cysteine. In the concentration range of  $1.08 \times 10^{-7}$ – $2.87 \times 10^{-6} \text{mol L}^{-1}$ ; the UV-Vis absorption had a linear relationship with Cys concentration. The regression equation was  $A_{545} = 0.4176 - 0.1113C_{\text{Cys}}$  ( $\mu\text{mol L}^{-1}$ ) with a correlation coefficient of 0.9978 (Fig. 3c). Based on the titration and linear relationship, the detection limit ( $3\delta/\text{slope}$ ) and the quantification limit ( $10\delta/\text{slope}$ ) of BPR- $\text{Mn}^{2+}$  toward Cys were calculated to be 0.02 and  $0.07 \mu\text{mol L}^{-1}$ , respectively.

Fig. 3c shows the absorbance as the concentration of L-cysteine ranges from 0.11 to  $2.87 \mu\text{mol L}^{-1}$ , which is a perfect linear relationship ( $R^2 = 0.9995$ ). Furthermore, a lower detection limit ( $20.0 \text{nmol L}^{-1}$ ) is addressed based on  $3\sigma$ , with comparison to previously reported L-cysteine determination methods [18–20, 39–43] (Table 2). In the meantime, the assay avoids any indirect, time-consuming problems and is convenient without any labels or complicated operations.

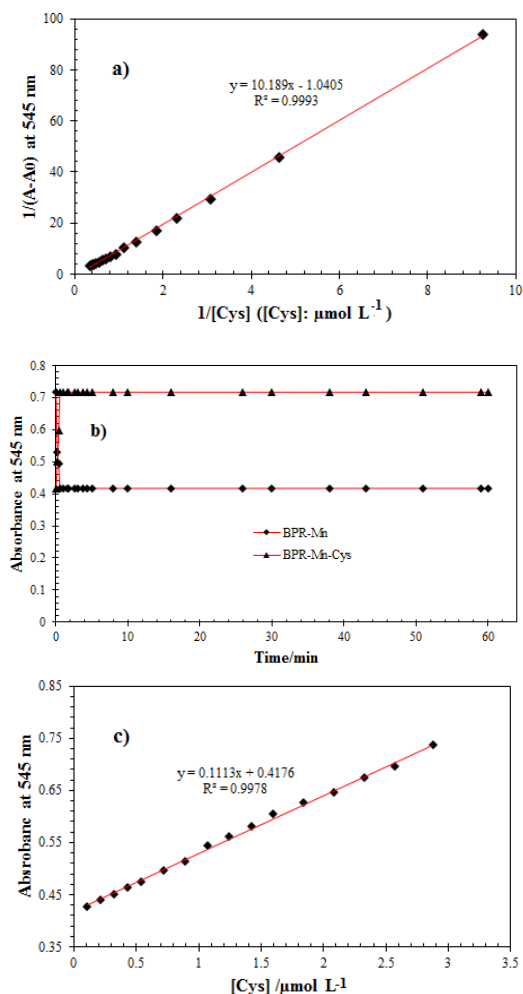


**Fig. 3.** a) Benesi-Hildebrand plot ( absorbance at 545nm) of BPR-  $Mn^{2+}$  (the variation of  $1/(A-A_0)$  at 545nm versus the function of  $1/[Cys]$ ) based on 1:1 binding stoichiometry with Cys b) Response time for the colorimetric detection of  $Mn^{2+}$  ( $30.0 \mu mol L^{-1}$ ) and Cys ( $30.0 \mu mol L^{-1}$ ) by BPR and BPR-  $Mn^{2+}$  receptors, respectively at 553 nm in EtOH/HEPES buffer  $10.0 mmol L^{-1}$ , pH 9.3 (1:4 v/v), c) The linearly proportional relationship between the absorbance of BPR-  $Mn^{2+}$  solution and the concentration of Cys at 545nm, in EtOH/HEPES buffer  $10.0 mmol L^{-1}$ , pH 9.3 (1:4 v/v).

### 3.4. Effect of pH

The predominant species of amino acids are highly pH-dependent since they incorporate both acidic and basic functional groups. As known, the pKa of  $\alpha-CO_2H$ ,  $\alpha-NH_3$ , and the S-H group of Cysteine are 1.96, 10.78, and 8.33, respectively [44]. Fig. 4a shows the protonation of the mentioned functional groups and the net charge of L-Cys in different pH values. As observed, under extremely acidic conditions,  $pH < 1.96$ , all carboxylate, thiol, and amine functional groups, are protonated, producing the net positive charged structure (cationic) for L-Cys. In the pH range  $1.96 < pH < 8.33$ , the thiol and amine groups are protonated while the carboxylic acid moiety sheds its proton.

At the characteristic pH value called isoelectric point (pI), negative and positive charges are equal, resulting in net-zero charges. The value of pI for Cys is calculated to be 5.14, the average of 1.96 and 8.33, using the Henderson-Hasselbalch equation [45].

In the pH range of  $8.33 < pH < 10.87$ , the negatively charged (anionic) structure is suggested because only the amine group is protonated at pHs greater than 10.8, everything is protonated to neutralize the rising OH-concentration. Over these circumstances, L-Cys has a doubly charged anionic structure. It is obvious in Fig. 4a that in the predominant structure at pH 7.0 just the carboxylic acid is protonated and the net charge of the structure is zero.

The IDAs-colorimetric response of the chemosensor in different pH values is presented in At high pH is consistent with L-cysteine forming the complex with manganese(II) [29]. Consequently, the proposed chemosensor is applicable at pH 9.3 which indicates that at this pH, Cys can form a stable complex with  $Mn^{2+}$  (Fig. 4b). To investigate the influence of different buffer solutions on the spectra of receptors, some experiments were performed to find a suitable pH span in which receptors can selectively and efficiently detect cation and amino acid ( $Mn^{2+}$  and Cys). As it is indicated in Fig. 4b, the addition of  $Mn^{2+}$  and Cys has the most obvious impact on the absorbance spectra over  $pH=9.3$ .

### 3.5. Selectivity of the developed indicator-displacement strategy for the detection of cysteine

To evaluate the selectivity of the developed indicator-displacement strategy for detecting cysteine, we studied the responses of the selective receptor, BPR- $Mn^{2+}$ , to 20 natural amino acids, and the biothiols cysteine (Cys) and glutathione (GSH). To further evaluate the applicability of the proposed colorimetric sensor for detecting cysteine in biological fluids, the interferences of other potential co-existing substances including magnesium, zinc, iron(III), potassium, calcium and sodium ions, glucose, urea, uric acid, and ascorbic acid, on the detection of cysteine was studied. Major species commonly found in biological matrices, for instance, did not affect the detection of  $60.0 \mu mol L^{-1}$  cysteine at the concentration level of  $200 \mu mol L^{-1}$  of the interferences. Fig. 2b shows that only cysteine led to significant changes in color and absorption spectra. The above results indicate good selectivity of the proposed replacement colorimetric sensor for cysteine over other natural amino acids and GSH in biological matrices. Color recovery induced by  $60.0 \mu mol L^{-1}$  of cysteine was not affected by interferences. The above results clearly show that the designed IDA protocol for cysteine has excellent selectivity for



detecting cysteine in biological fluids. More importantly, this system is very convenient for qualitative and quantitative detection.

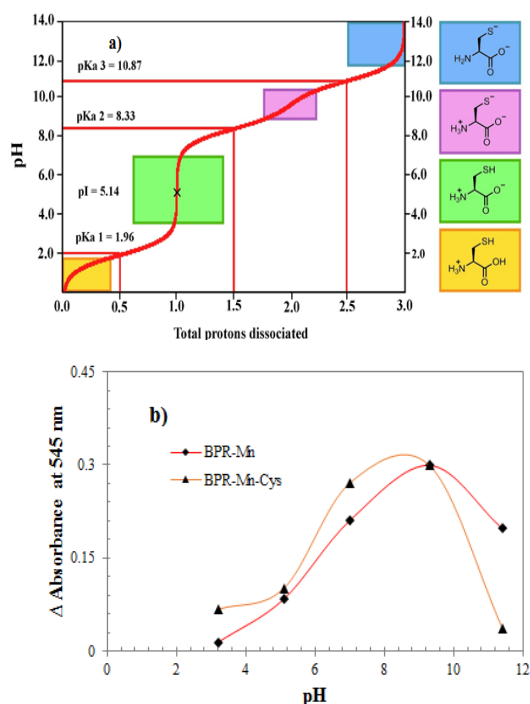


**Fig. 4.** a) The graph of net charge and predominant structure of L-Cysteine in different pH values a) Effect of the pH on the absorbance changes of BPR ( $30.0 \mu\text{mol L}^{-1}$ ) in the presence of  $\text{Mn}^{2+}$  ( $30.0 \mu\text{mol L}^{-1}$ ) and [BPR- $\text{Mn}^{2+}$ ] complex in the presence of Cys ( $30.0 \mu\text{mol L}^{-1}$ ) at 545 nm in EtOH/HEPES buffer  $10.0 \text{ mmol L}^{-1}$ , pH 9.3 (1:4 v/v).

### 3.6. Reversibility of the chemosensor

The development of reversibly colorimetric chemosensors for amino acid determination with high sensitivity and selectivity is highly desirable. The reversibility of the chemosensor is an important aspect of its practical applications. Considerably, in this work the imposed spectral and color changes in the produced chemosensor are reversible. The addition of Cys ( $60.0 \mu\text{mol L}^{-1}$ ) results in the disappearance of the absorption band of the BPR- $\text{Mn}$  complex at 545 nm. As observed in Fig. 5, in a cyclic process, serial addition of  $\text{Mn}^{2+}$  and Cys induces reappearance and disappearance of the absorbance band centered at 545nm, respectively.

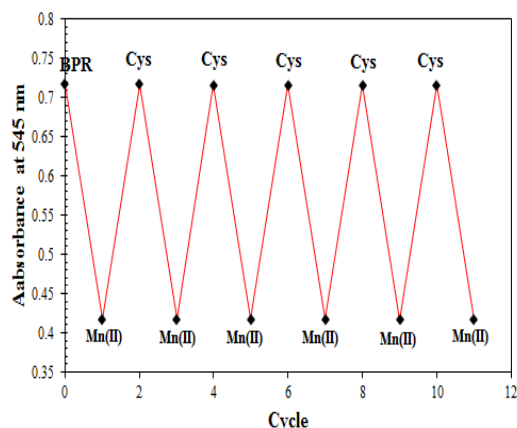


**Fig. 5.** The reversible and reproducible absorption signal at 545 nm imposed by alternate addition of  $\text{Mn}^{2+}$  ( $30.0 \mu\text{mol L}^{-1}$ ) and Cys ( $60.0 \mu\text{mol L}^{-1}$ ) into the BPR solution ( $30.0 \mu\text{mol L}^{-1}$ ) in EtOH/HEPES buffer  $10.0 \text{ mmol L}^{-1}$ , pH 9.3 (1:4 v/v).

**Table 2.** Evaluation of analytical features of the reported colorimetric chemosensor in comparison with the recently reported colorimetric methods for Cys determination

Ref.	LOD ( $\mu\text{mol L}^{-1}$ )	Linear range ( $\mu\text{mol L}^{-1}$ )	pH range	Response time	Water content of solution (%)
[39]	1.0	4.0-94.0	9.0	2 min	100
[40]	10.77	No Data	No Data	No Data	50
[41]	0.18	0-25	8-9	15 min	60
[42]	0.99	10-100	No Data	10 min	100
[43]	0.003	0.01-0.17	3-9	5 min	100
[18]	0.07	0.6-25.8	5-10	Less than 30 s	100
[19]	0.35	2.25-42.91	6-10	Less than 30 s	70
[20]	1.33	5.23-95.5	6-9	Less than 30 s	100
Presented work	0.02	0.11-2.78	9.3	Less than 30 s	80

### 3.7. Logic gate construction of the proposed colorimetric chemosensor

Lately, variant Boolean logic operations with applications for biosensors and bioimaging have been developed [46]. Here, the proposed probe inspires us to fabricate IMPLICATION molecular logic gates to prove its feasible application in the future. If the remarkable characteristics are attended on the response of the optical signal of this chemosensor,  $Mn^{2+}$  and Cys as two inputs for the IMPLICATION gate are employed. The absence and presence of the inputs are respectively described as "0" and "1".

IMPLICATION gate was obtained to peruse the absorbance behavior of BPR in response to  $Mn^{2+}$  and Cys (Fig. 6 and Truth Table). The output is the specific value of  $A_{545nm}$ . There are four different states of the presence and/or absence of  $Mn^{2+}$  ions and Cys, namely (0, 0) (1, 0) (0, 1), and (1, 1). Only in the presence of  $Mn^{2+}$  and the absence of Arg, the output is 0 due to the specific combining between BPR and  $Mn^{2+}$  for complex formation. However, the presence of Cys resulted in a higher specific value of  $A_{545nm}$  ( $A_{545nm} > 0.42$  au), indicating that a typical IMPLICATION logic gate can be created for the determination of Arg.

Truth Table		
INPUTS		OUTPUT
$Mn^{2+}$	Cysteine	Absorbance at 545nm (IMPLICATION) gate
0	0	1(High)
0	1	1(High)
1	0	0(Low)
1	1	1(High)

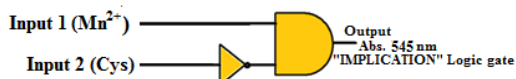
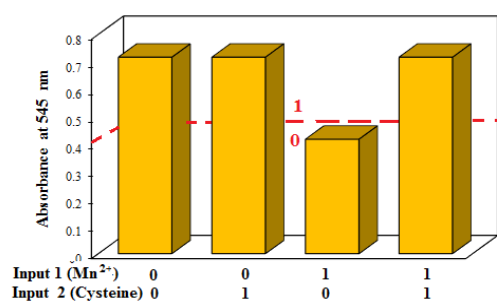


**Fig. 6.** Illustration of "IMPLICATION" logic gate: The histogram of different inputs values based on UV-Vis absorption at 545 nm, and truth table corresponding to the "IMPLICATION" logic gates. The complementary "IMPLICATION" logic gate and its truth table INP1 and INP2 represent Input  $Mn^{2+}$  and Input Cys, respectively.

### 3.8. The chemosensory system as a keypad lock

According to the response of the BPR chemosensor to  $Mn^{2+}$  and Cys, this system was

investigated as a keyboard lock, and the absorption behavior of BPR was observed during the successive addition of these two inputs. The first input sequence,  $Mn^{2+}$  as input 1 and excess Cys ( $90.0 \mu\text{mol L}^{-1}$ ) as input 2 resulted in a increase in absorbance from 0.42 to almost 0.72 at 545 nm (Fig. 1a and Fig. 2b). After reversing the chemical inputs, Cys as input 1 and  $Mn^{2+}$  as input 2, the absorbance value at 545 nm increases from 0.72 to 0.42 (Fig. 5).

As a result, the sequence of adding  $Mn^{2+}$  and Cys to the BPR solution leads to changes (increase/decrease) in the absorbance value at 545 nm. If the order of the inputs is reversed, the repeated output (ON) will not be developed. According to the above consequence about the absorption outputs, it has been concluded that we can design our system as a security keyboard unlock. To produce the input sequence as the password and the BPR chemosensor as the keyboard unlock, the  $Mn^{2+}$  and Cys inputs were marked as "M" and "C", respectively (Fig. 7). For the first input sequence, "M" followed by "C" consequence in "ON" absorption at 545 nm, creating a secret code "MCT" where "T" defines the "ON" state. In reversing the input sequence, i.e., first input "C" followed by "M", absorbance was in the "OFF" state at 545 nm. Consequently, this sequence i.e., "CMF", where "T" describes the "OFF" state, is a wrong input and is not able to lock the keyboard. We confirm that a "CMF" security code has been generated that can be used to lock BPR absorption at 545 nm.

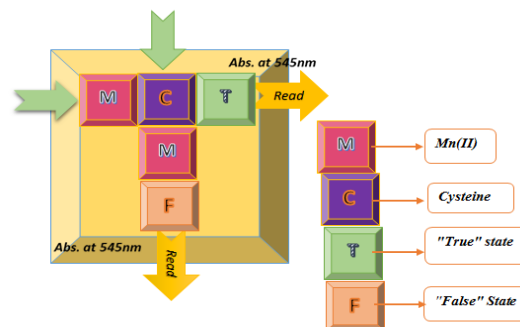


**Fig. 7.** Absorbance keypad locks with the inputs of  $Mn^{2+}$  and Cys to access a secret code at 545 nm.

### 3.9. $Mn^{2+}$ and L-cysteine detection assay in real samples

As an essential bioactive amino acid component of many proteins, the detection of cysteine in biological fluids such as urine and plasma is in urgent demand. With previous results in hand, we explored the quantitative determination of cysteine in plasma samples using the BPR-Mn ions receptor. We studied the colorimetric response of receptors to Cys in the presence of some biological species, including magnesium, zinc, iron(III), potassium, calcium and sodium ions, glucose, urea,

uric acid and ascorbic acid (Fig. 2b). No obvious absorbance changes of BPR-Mn<sup>2+</sup> in the presence of Cys were observed when these biological species were added, indicating the potential utility of receptors for the determination of Cys in biological fluids. Then, plasma and urine were diluted 150 and 15 times respectively, before use. The analysis results which are summarized in Table 3 appeared to be comparable with the results from the reference method (HPLC method) [31], there were not any statistically significant differences by *t*-test [47] (95% confidence interval and *n* = 4). Therefore, the use of this sensor in the application of real samples was accredited with high sensitivity.

The concentrations of manganese(II) ions in the spiked artificial water samples determined by the developed method were in good agreement with those of the added Mn<sup>2+</sup>. A summary of the spiked concentration for each sample and the corresponding analysis results are shown in Table 4. The quantitative recoveries ranged from 97.3% to 104.0%, which indicated that the present method is promising in practical applications with great accuracy and reliability.

**Table 3.** Determination of Cys in biological fluid ( $\mu\text{mol L}^{-1}$ ) by using the proposed method and reference method (Mean Value<sup>1</sup>  $\pm$  Standard Deviation).

Sample <sup>a</sup>	Cys ( $\mu\text{mol L}^{-1}$ )		Critical t
	Proposed Method	Reference Method <sup>b</sup>	
Human plasma <sup>c</sup>	263.8	265.1	1.24
Human Urine <sup>d</sup>	24.6	24.1	0.84

<sup>a</sup> Relative standard deviation of 5 individual measurements

<sup>b</sup> HPLC method [31]

<sup>c</sup> Value determined after 150 times dilution

<sup>d</sup> Value determined after 15 times dilution

**Table 4.** Determination of manganese ion ( $\mu\text{mol L}^{-1}$ ) in water samples by using the proposed method (Mean Value<sup>1</sup>  $\pm$  Standard Deviation).

Sample	Mn <sup>2+</sup> ( $\mu\text{mol L}^{-1}$ )		Recov ery (%)	RSD <sup>b</sup> %
	Added	Found <sup>a</sup>		
Runn ing water	0.0	ND <sup>b</sup>	—	—
	5.0	5.2 $\pm$ 0.1	104.0	1.33
	10.0	9.8 $\pm$ 0.3	98.0	0.98
	15.0	14.6 $\pm$ 0.4	97.3	2.25
Tap water	0.0	ND	—	—
	5.0	5.1 $\pm$ 0.2	102.0	2.01
	10.0	10.3 $\pm$ 0.1	103.0	1.36
	15.0	14.8 $\pm$ 0.5	98.6	1.25

<sup>a</sup> Relative standard deviation of 5 individual measurements

<sup>b</sup> ND cannot be determined using the spectra

## CONCLUSIONS

Since the lack or change in the level of cysteine in the body leads to liver and skin diseases, Alzheimer's, neurotoxicity, developmental delay in children, weak immune system, cancer in severe cases, etc., therefore measuring its level in the human body is very important. It is necessary and important. In the present study, a new type of label-free, rapid, highly selective, and sensitive colorimetric method was developed that can sequentially measure Mn<sup>2+</sup> ion and cysteine colorimetrically with high selectivity and sensitivity compared to other ions/acids. Competitive amines can be detected in 80% of water media. The BPR-Mn<sup>2+</sup> complex can be successfully applied to biological samples for the detection of cysteine. First of all, this protocol provides high selectivity for the determination of Cys among amino acids in proteins as well as their detection in human plasma and urine samples, secondly, selective detection of a specific amino acid without interference from other amino acids of a matrix. It is complicated. The proposed BPR probe was used to make IMPLICATION a logic gate. Eventually, based on such a fast, reversible, and reproducible signal, a molecular-scale sequential memory unit was designed to display "keypad lock" behavior. Based on the results, the BPR receptor provides important guidance in the development of a single receptor for the detection of multiple analytes. This new method eliminated the need for separation processes, modification of chemical and organic solvents, instrumentation, and enzymatic reactions.

## SUGGESTIONS FOR FUTURE WORK:

The assessment showed great potential for practical applications as a disease-associated biomarker and would be needed to amuse the great claim of amino acid determination in fields such as biochemistry, food processing, pharmaceuticals, and clinical analysis. Accordingly, as many biomolecules could form stable complexes with metal ions selectively, these findings offer the potential to come close to the detection of a wide range of analytes.

## ACKNOWLEDGEMENTS

The authors wish to acknowledge the support of this work by Shiraz Payame Noor University Research Council with grant IDs d/7/47416 and Layout code 3146. The authors also wish to acknowledge Dr Gohar Deilamy-Rad.

## REFERENCES

- [1] W. Ngeontae, K. Chaiendoo, K. Ngamdee, S. Ruangchai, C. Saiyasombat, W. Busayaporn, S. Ittisanronnachai, and V. Promarak, A highly selective fluorescent sensor for manganese (II) ion detection based on N, S-

- doped carbon dots triggered by manganese oxide, *Dye. Pigment.* 203 (2022) 110325.
- [2] J. Park, M. B. Cleary, D. Li, J. A. Mattocks, J. Xu, H. Wang, S. Mukhopadhyay, E. M. Gale, and J.A. Cotruvo Jr, *Proc. Natl. Acad. Sci.* 51 (2022) e2212723119.
- [3] W. Zou, J. Li, and X. Gong, A facile synthetic strategy to simultaneously achieve ultra-wide PL redshift of carbon nanodots and their high selectivity and sensitivity for Mn<sup>2+</sup> detection, *Mater. Today Chem.* 37 (2024) 102001.
- [4] F. Mollaamin, and M. Monajjemi, Determination of GaN nanosensor for scavenging of toxic heavy metal ions (Mn<sup>2+</sup>, Zn<sup>2+</sup>, Ag<sup>+</sup>, Au<sup>3+</sup>, Al<sup>3+</sup>, Sn<sup>2+</sup>) from water: Application of green sustainable materials by molecular modeling approach, *Comput. Theor. Chem.* 1237 (2024) 114646.
- [5] P. D. Singh, Z. V. Murthy, and S. K. Kailasa, Zinc nitride quantum dots as an efficient probe for simultaneous fluorescence detection of Cu<sup>2+</sup> and Mn<sup>2+</sup> ions in water samples, *Microchim. Acta.* 191(2024) 161.
- [6] X. Dai, C. Song, S. Ma, F. Cao, and D. Dong, Rapid Determination of Cr<sup>3+</sup> and Mn<sup>2+</sup> in Water Using Laser-Induced Breakdown Spectroscopy Combined with Filter Paper Modified with Gold Nanoclusters, *Biosens.* 14 (2024) 267.
- [7] S. Rayati, Y. D. Farahani, and J. B. Ghasemi, Surface decorated graphene oxide with porphyrin: A Promising On-off sensor for Mn<sup>2+</sup> ions detection in aqueous media, *J. Mol. Struct.* (2024)138897.
- [8] V. Raju, R. S. Kumar, Y. Tharakeswar, and S. A. Kumar, A multifunctional Schiff-base as chromogenic chemosensor for Mn<sup>2+</sup> and fluorescent chemosensor for Zn<sup>2+</sup> in semi-aqueous environment, *Inorganica Chim. Acta.* 493 (2019)49-56.
- [9] Y. Yu, Y. Li, Q. Zhang, Y. Zha, S. Lu, Y. Yang, P. Li, and Y. Zhou, Colorimetric immunoassay via smartphone based on Mn<sup>2+</sup>-Mediated aggregation of AuNPs for convenient detection of fumonisin B1, *Food Control.* 132 (2022)108481.
- [10] A. Dinu, and C. Apetrei, A review of sensors and biosensors modified with conducting polymers and molecularly imprinted polymers used in electrochemical detection of amino acids: Phenylalanine, tyrosine, and tryptophan, *Int. J. Mol. Sci.* 23 (2022) 1218.
- [11] R. Kumar, G. B.V. S. Lakshmi, K. Singh, and P.R. Solanki, A novel approach towards optical detection and detoxification of Cr (VI) to Cr (III) using L-Cys-VS2QDs, *J. Environ. Chem. Eng.* 7 (2019) 103202.
- [12] B. P. Jagilinki, S. Ilic, C. Trncik, A.M. Tyryshkin, D.H. Pike, W. Lubitz, E. Bill, O. Einsle, J. A. Birrell, B. Akabayov, D. Noy, and V. Nanda, In vivo biogenesis of a de novo designed iron-sulfur protein, *ACS Synth. Biol.* 9 (2020) 3400-7.
- [13] J. A. Combs, and G. M. Denicola, The non-essential amino acid cysteine becomes essential for tumor proliferation and survival, *Cancers* 11 (2019) 678.
- [14] D. Rohilla, S. Chaudhary, N. Kaur, and A. Shanavas, Dopamine functionalized CuO nanoparticles: A high valued “turn on” colorimetric biosensor for detecting cysteine in human serum and urine samples, *Mater. Sci. Eng. C* 110 (2020) 110724.
- [15] F. Yan, X. Sun, F. Zu, Z. Bai, Y. Jiang, K. Fan, and J. Wang, Fluorescent probes for detecting cysteine. Methods and applications in fluorescence, *Methods Appl. Fluoresc.* 6 (2018) 042001.
- [16] N. Cao, H. Zhou, H. Tan, R. Qi, J. Chen, S. Zhang, and J. Xu, Turn-on fluorescence detection of cysteine with glutathione protected silver nanoclusters, *Methods Appl. Fluoresc.* 7 (2019) 034004.
- [17] Z. Huang, C. Wu, Y. Li, Z. Zhou, R. Xie, X. Pang, H. Xu, H. Li, and Y. Zhang, A fluorescent probe for the specific detection of cysteine in human serum samples, *Anal. Methods* 11 (2019) 3280-5.
- [18] H. Tavallali, G. Deilamy-Rad, M. A. Karimi, and E. Rahimy A novel dye-based colorimetric chemosensors for sequential detection of Cu<sup>2+</sup> and cysteine in aqueous solution, *Anal. Biochem.* 583 (2019) 113376.
- [19] G. Deilamy-Rad, K. Asghari, and H. Tavallali, Development of a reversible indicator displacement assay based on the 1-(2-Pyridylazo)-2-naphthol for colorimetric determination of cysteine in biological samples and its application to constructing the paper test strips and a molecular-scale set/reset memorized device, *Appl. Biochem. Biotechnol.* 192 (2020) 85-102.
- [20] H. Tavallali, G. Deilamy-Rad, and N. Mosallanejad, Reactive blue 4 as a Single colorimetric chemosensor for sequential determination of multiple analytes with different optical responses in aqueous media: Cu<sup>2+</sup>-cysteine using a metal ion displacement and Cu<sup>2+</sup>-arginine through the host-guest interactionAppl, *Biochem. Biotechnol.* 187 (2019) 913-37.
- [21] T. K. Stewart, I. E. Carotti, Y. M. Qureshi, and J. A. Covington, Trends in chemical sensors for non-invasive breath analysis, *TrAC, Trends Anal. Chem.* 25 (2024) 117792.
- [22] H. Tavallali, G. Deilamy-Rad, A. Parhami, K. Asghari, and A. Ahmadi, Bismuth triggered selective colorimetric naked-eye detection for

- oxalate ions based on bromopyrogallol red that works as a molecular keypad lock, *J. Environ. Anal. Chem.* 101(2021) 648-67.
- [23] H. Tavallali, S. Fakhraee, M. Dashti Darvishzadeh, M.A. Karimi, and E. Rahimi, Colorimetric detection of clotrimazole environmental pollutant using a newly developed chemosensor; an experimental and theoretical study, *J. Environ. Anal. Chem.* (2024) 1-19.
- [24] H. Tavallali, G. Deilamy-Rad, A. Parhami, and E. Abbasiyan, A novel and efficient colorimetric chemosensor for detection and determination of biologically important ions in DMSO/H<sub>2</sub>O media using bromo pyrogallol red chemosensors with analytical applications, *J. Photochem. Photobiol. B.* 115 (2012) 51-7.
- [25] H. Tavallali, G. Deilamy-Rad, A. Parhami, and E. Abbasiyan, Colorimetric detection of copper and chloride in DMSO/H<sub>2</sub>O media using bromopyrogallol red as a chemosensor with analytical applications, *Spectrochim. Acta Part A Mol. Biomol. Spectrosc.* 97 (2012) 60-5.
- [26] B. Das, and P. Gupta, Multimetallic transition metal complexes: Luminescent probes for biomolecule sensing, ion detection, imaging and therapeutic application, *Coord. Chem. Rev.* 504 (2024) 215656.
- [27] H. Tavallali, G. Deilamy-Rad, A. Parhami, and N. Hasanli, An efficient and ultrasensitive rhodamine B-based reversible colorimetric chemosensor for naked-eye recognition of molybdenum and citrate ions in aqueous solution: Sensing behavior and logic operation, *Spectrochim. Acta Part A Mol. Biomol. Spectrosc.* 139 (2015) 253-61.
- [28] H. Tavallali, M. R. Baezzat, G. Deilamy-Rad, A. Parhami, and N. Hasanli, An ultrasensitive and highlyselective fluorescent and colorimetric chemosensor for citrate ions based on rhodamine B and its application as the first molecular security keypad lock based on phosphomolybdic acid and citrate inputs, *J. Lumin.* 60 (2015) 328-36.
- [29] R. K. Boggess, J. R. Absher, S. Morelen, L.T. Taylor, and J. W. Hughes, Interaction of manganese (II) and amino acids with emphasis on cysteine and penicillamine (beta., beta.-dimethylcysteine), *Inorg. Chem.* 22 (1983) 1273-9.
- [30] H. Tavallali, G. Deilamy-Rad, A. Parhami, and S. Kiyani, Dithizone as novel and efficient chromogenic probe for cyanide detection in aqueous media through nucleophilic addition into diazenylthione moiety, *Spectrochim. Acta A Mol. Biomol. Spectrosc.* 121 (2014) 139-46.
- [31] W. Chen, Y. Zhao, T. Seefeldt, and X. Guan, Determination of thiols and disulfides via HPLC quantification of 5-thio-2-nitrobenzoic acid, *J. Pharm. Biomed. Anal.* 48 (2008) 1375-80.
- [32] H. A. Benesi, and J. H. Hildebrand, A Spectrophotometric Investigation of the Interaction of Iodine with Aromatic Hydrocarbons, *J. Am. Chem. Soc.* 71 (1949) 2703-07.
- [33] Y. Fukushima, and S. Aikawa, Colorimetric detection of Mn (II) based on a mixture of an anionic pyridylazo dye and a cationic polyelectrolyte in aqueous solution, *Color. Technol.* 136 (2020) 450-6.
- [34] Y. Wang, X. Wang, K. Zhang, X. Wang, X. Xin, W. Fan, F. Dai, Y. Han, and D. Sun, Solvent-induced terbium metal-organic frameworks for highly selective detection of manganese (II) ions, *Dalton Trans.* 48 (2019) 2569-73.
- [35] L. Zhao, H. Li, H. Liu, M. Liu, N. Huang, Z. He, Y. Li, Y. Chen, and L. Ding, Microwave-assisted facile synthesis of polymer dots as a fluorescent probe for detection of cobalt (II) and manganese (II), *Anal. Bioanal. chem.* 411 (2019) 2373-81.
- [36] N. Roy, A. Dutta, P. Mondal, P. C. Paul, and T.S. Singh, A new turn-on fluorescent chemosensor based on sensitive Schiff base for Mn<sup>2+</sup> ion, *J. Lumin.* 165 (2015) 167-73.
- [37] Y. J. Lee, C. Lim, H. Suh, E. J. Song, and C. Kim, A multifunctional sensor: chromogenic sensing for Mn<sup>2+</sup> and fluorescent sensing for Zn<sup>2+</sup> and Al<sup>3+</sup>, *Sensor Actuat. B-Chem.* 201 (2014) 535-44.
- [38] C. W. Ooi, U. Waldo, Y. Norazriena, , K. S. Lim, S. T. Tan, Z. Rozalina, and H. Ahmad, L-cysteine grafted fiber-optic chemosensor for heavy metal detection, *Opt. Fiber Technol.* 71 (2022) 102938.
- [39] H. Khajehsharifi, and A. Sheini, A selective naked-eye detection and determination of cysteine using an indicator-displacement assay in urine sample, *Sensor Actuat. B-Chem.* 199 (2014) 457-62.
- [40] S. A. Lee, J. J. Lee, J. W. Shin, K. S. Min, and C. Kim, A colorimetric chemosensor for the sequential detection of copper (II) and cysteine, *Dyes Pigm.* 116 (2015) 131-8.
- [41] S. Xue, S. Ding, Q. Zhai, H. Zhang, and G. Feng, A readily available colorimetric and near-infrared fluorescent turn-on probe for rapid and selective detection of cysteine in living cells, *Biosens. Bioelectron.* 68 (2015) 316-21.
- [42] X. Wei, L. Qi, J. Tan, R. Liu, and F. Wang, A colorimetric sensor for determination of cysteine by carboxymethyl cellulose-functionalized gold nanoparticles, *Anal. Chim. Acta* 671 (2010) 80-4.

- [43]K. Farhadi, M. Forough, A. Pourhossein, and R. Molaei, Highly sensitive and selective colorimetric probe for determination of l-cysteine in aqueous media based on Ag/Pd bimetallic nanoparticles, *Sensor Actuat. B-Chem.* 202 (2014) 993–1001.
- [44]J. M. Berg, J. L. Tymoczko, and L. Stryer, Biochemistry, *Fifth Edition: W.H. Freeman*, (2002).
- [45]D. A. Skoog, D. M. West, F. J. Holler, and S. R. Crouch, Fundamentals of Analytical Chemistry, *Cengage Learning*, (2013).
- [46]L. Feng, Z. Lyu, A. Offenhausser, and D. Mayer, Multi-level logic gate operation based on amplified aptasensor performance, *Angew. Chem. Int. Edit.* 54 (2015) 7693–7.
- [47]T. K. Kim, T test as a parametric statistic, *Korean. J. Anesthsioal* 68 (2015) 540-6.



#### COPYRIGHTS

© 2022 by the authors. Lisensee PNU, Tehran, Iran. This article is an open access article distributed under the terms and conditions of the Creative Commons Attribution 4.0 International (CC BY4.0) (<http://creativecommons.org/licenses/by/4.0>)

## یک حسگر شیمیایی امیدوارکننده بر پایه کمپلکس منگنز (II) با یک لیگاند زانتن به عنوان یک رنگ تجاری در دسترس برای تشخیص سیستمین در نمونه‌های بیولوژیکی

حسین توللی\*، حسام الدین حقدان

بخش شیمی، دانشگاه پیام نور، تهران، ایران

\* E-mail: [Tavallali@pnu.ac.ir](mailto:Tavallali@pnu.ac.ir), [Tavallali@yahoo.com](mailto:Tavallali@yahoo.com)

تاریخ دریافت: ۹ شهریور ۱۴۰۳ تاریخ پذیرش: ۱۶ شهریور ۱۴۰۳

### چکیده

در این مطالعه، یک حسگر شیمیایی رنگ سنجی جدید برای تشخیص و تعیین منگنز (II) و سیستمین (Cys) با چشم غیر مسلح بر اساس سنجش جابجایی شناساگر (IDA) با استفاده از بومو پیوگالول قرمز (BPR) طراحی و توسعه داده شد. تبادل بین BPR و Cys با افزودن Cys به کمپلکس منگنز-BPR رخ داد که منجر به تغییر رنگ واضح و سریع از بنفش به سرخابی در محیط اتانول /محلول ۱۰/۰ میلی مولار بافر HEPES در pH=۹/۳ با نسبت حجمی/حجمی ۴:۱ همراه بود. روش پیشنهادی حد تشخیص ۰/۰۲ میکرومول بر لیتر و محدوده خطی ۰/۲-۱۱/۸۷ میکرومول بر لیتر برای سیستمین را نشان می دهد. علاوه بر این، بر اساس تغییرات جذب ایجاد شده و تغییر رنگ مشاهده شده، این حسگر شیمیایی به عنوان یک دروازه منطقی "IMPLICATION" با در نظر گرفتن منگنز (II) و Cys به عنوان ورودی پیشنهاد شده است. به عنوان یک کاربرد در اندازه های مولکولی، بر اساس چنین سیگنال سریع و قابل تکرار، یک واحد حافظه متوالی در مقیاس مولکولی برای نشان دادن رفتار "قفل صفحه کلید" طراحی شده است. حسگر شیمیایی توسعه یافته تکرارپذیری رضایت بخش، دقت خوب و کاربرد موفقیت آمیز را برای تعیین انتخابی Cys در مایعات بیولوژیکی انسان فراهم می کند. همچنین دقت روش با مقایسه نتایج به دست آمده از روش پیشنهادی و روش مرجع مورد ارزیابی قرار گرفت.

### کلید واژه ها

سنجش جابجایی نشانگر (IDA)، حسگر شیمیایی رنگ سنجی، منگنز (II)، سیستمین، بومو پیوگالول قرمز (BPR)، قفل صفحه کلید مولکولی.